2013-01-01

Polymer micro-grippers with an integrated force sensor for biological manipulation

Mackay, RE

http://hdl.handle.net/10026.1/3261

10.1088/0960-1317/23/1/015005
JOURNAL OF MICROMECHANICS AND MICROENGINEERING
IOP Publishing

Published in J. Micromech. Microeng. **23** (2013) 015005, doi:10.1088/0960-1317/23/1/015005

Polymer micro-grippers with an integrated force sensor for biological manipulation

R E Mackay[1*, 3], H R Le[2], S Clark[3], J A Williams[4]

[1*] Correspondent Author: Centre for Electronic Systems Research, School of Engineering and Design, Brunel University, Uxbridge, Middlesex. U.K. E-mail: ruth.mackay@brunel.ac.uk

[2]School of Marine Science and Engineering, Plymouth University, Plymouth, U.K. Email: huirong.le@plymouth.ac.uk

[3]School of Engineering, Physics and Mathematics, University of Dundee, Dundee, U.K.

[4]Department of Engineering, Trumpington Street, University of Cambridge, Cambridge, U.K. Email: jaw1000@cam.ac.uk

Abstract. The development of a novel system integrating SU-8 micro-grippers with a tensile force sensor for handling and characterising the mechanical properties of delicate biological samples, such as fibrils, is presented. The micro-grippers are actuated by the electro-thermal effect and have gripping forces comparable to the common "hot-and-cold-arm" grippers. A thorough and robust finite element model was developed for design optimisation and validated experimentally. A new micro-mechanical calibration method using a piezoelectric manipulator with a force measurement system was successfully applied to test the structure.

Keywords. MEMS, Microgripper, Tensile force sensor, SU-8

1. Introduction

Cells and tissues are constantly responding to mechanical stimuli that produce chemical responses which can influence many aspects of behaviour such as cellular growth, differentiation and adhesion. Mechanical characterisation of small-scale tissue volumes can be important in enhancing our understanding some of these aspects of fundamental cell physiology [1]. For example, mechanical stimulation of developing artificial tissue has been shown to create 3-D tissues with improved mechanical properties [2]. On the other hand, it has been found that mechanical forces may be responsible for angiogenesis, i.e. the formation of new blood vessels, previously thought to be due to chemical signalling which can represent a bottleneck for tissue engineers trying to create large-scale tissue samples [3].

Several designs of micro-grippers capable of mechanically handling individual cells and small tissue volumes have been developed [4] and when integrated with a means of force sensing these can be used to investigate tissue compliance or hardness [5]. A number of MEMS/NEMS (Micro/NanoElectroMechanical Systems) have been developed to study these biomechanical properties although these are usually designed for very specific applications, e.g. heart cell force transduction or *in vivo* tissue hardness tests [6,7]. Force sensing can be conveniently carried out optically by measuring the displacements of compliant mechanisms with known stiffnesses [8].

A variety of MEMS actuation methods have been described in the literature including electrostatic, piezo-electric, electro-thermal and the use of shape memory alloys [8-14]. Electro-thermal micro-grippers have the advantage over other devices of acceptably low actuating voltages and careful material selection can allow the temperature increases to be small enough to avoid damage to biological samples. Chronis and Lee [15] developed polymer micro-tweezers for cellular handling that were actuated using an underlying metallic layer as the conductor using a 'hot-and-cold-arm' technique [15]. The micro-grippers were fabricated using SU-8 as the main structural material and an underlying chromium adhesion layer and gold conduction path were used to pass current through the micro-gripper arms. SU-8 was chosen as the structural material because of its good biocompatibility and comparatively high coefficient of thermal expansion. The micro-gripper arms were 650 μm long and the maximum displacement was 15 μm. The gripping force is not stated but small beads were successfully manipulated. Luo et al. [16] conducted a study of the displacements and temperature increases of three types of nickel based electro-thermal micro-tweezers. For any given power input their Type III micro-tweezers showed the highest displacement with the lowest temperature increase largely because, with designs of this type, actuation only occurs in the gripping plane.

Biocompatibility and handling temperature are important considerations when designing instruments for manipulating biological tissues as both can cause premature cell death [15]. High voltages in electrolytic media can cause bubble formation and so parasitic movement of the samples to be grasped. The polymer SU-8 was chosen in this work as the principal material because of its biocompatibility, low operating temperatures and high coefficient of thermal expansion. The design of the micro-grippers themselves was based on a Luo et al Type III configuration [16] modified to include a mechanical/optical force sensor to facilitate tissue characterisation. The design concept, robust finite element model and low cost fabrication technique are outlined in the following sections. The observed operation of the micro-grippers is described as is its mechanical characterisation which was investigated using a Kleindiek piezoelectric micromanipulator.

2 . Design Concept

The design concept of the micro-grippers is shown in Fig. 1. To operate the grippers, current is passed from one contact pad to the other through a chromium conduction path which lies immediately beneath the SU-8 polymer layer. Between the L-shaped anchor points the conduction path is both of thinner section and free of the underlying substrate so that its expansion, due to Joule heating, leads to the opening of the micro-gripper tips. When the current is switched off, rapid cooling leads to closure of the gripper tips so grasping the specimen. If now this is subjected to a mechanical tensile force, normal to the gripping force, then this will be equilibrated by an equal and opposite force generated by bending of the two symmetrical folded flexures as the shuttle moves incrementally from left to right. The small silicon mirror incorporated at the left hand end of the shuttle can, in principle, be used to monitor the movement of the shuttle and thus, from a knowledge of the compliance of the flexural elements, to monitor the magnitude of the tensile load applied to the gripped specimen. The corresponding fibre optic displacement sensor would be mounted off-chip [17].

The micro-gripper and compliant spring structure were fabricated in SU-8 2007 negative photoresist which has a comparatively high coefficient of thermal expansion, viz. $52 \times 10^{-6}\,\mathrm{K}^{-1}$, and a low Young's modulus of $4.02\,\mathrm{GPa}$ [18]. Theoretical calculations were used to estimate micro-gripper tip displacement, gripping stiffness and maximum gripping force, the spring stiffness of the hot arms, the compliance of the folded flexures and the maximum stresses and temperature increases.

Table 1. Material properties and dimensions for the proposed micro-gripper structure

Young's Modulus	E	4.02 GPa
Maximum stress	s_f	34 MPa
Beam thickness	b	50 µm
Beam width	d	20 µm
Total length of gripping arm length	L_T	2 mm
Length of thin section of griping arm	L_1	45 µm

The gripping stiffness k_{grip}, i.e. the value relevant to forces applied in a direction normal to the gripper faces, can be estimated from expression (1) below which is based on treating each of the gripping jaws as a simple structural cantilever of varying section; this assumes that the hinges have minimal bending resistance and the bending of the thick section is negligible so that the arm rotation is determined by the deformation of the thinner section [16]

$$k_{grip} = \frac{EI_1}{L_1\left(L_T^2 + L_T L_1 + L_1^2/3\right)} \tag{1}$$

Here E is the Young's modulus of SU-8, L_1 and I_1 are the length and second moment of area of the thinner section and L_T is the total length of the gripping arm as indicated in Fig. 2. For the dimensions chosen and a structural layer thickness of 50 µm and element width of 20 µm, this gives a gripping stiffness of ca. $4.7\ \mathrm{Nm}^{-1}$. Thus the micro-grippers would generate a gripping force of 1 mN if each gripper arm was displaced by around 210 µm. If the gripper arm is treated as a simple encastré cantilever, then the maximum force $F_{\max}$ that can be applied safely at the tip of the micro-gripper is related to the maximum allowable stress in the material s_f by eqn. (2) [19, 20].

$$F_{\max} = \frac{s_f b d^2}{6L_T} \tag{2}$$

where b is the width of the beam and d is the thickness of the material.

The stiffness of the folded beam flexure which constitutes the force sensor has been examined in a previous publication [21] but its stiffness $k_{flexure}$ can be expressed by a similar expression to eqn. (1) above.

Because of the multi-physical nature of the problem, the failure mechanism of the structure may be more complex than eqn. (2) suggests and involve a combination of factors such as overheating of the hot arms and mechanical failure of the flexural hinges. ANSYS multi-physics Finite Element Analysis was used to model the structure allowing for the coupling of the thermal, electrical and mechanical aspects of the design by using ANSYS Solid 98 elements. Simulations were carried out with the device assumed to be operating in air at an ambient temperature of 25°C. Attachment to the substrate was mimicked by providing restraints in *x, y* and *z* directions at the anchor points and the grippers were displaced by applying forces at the centre of the gripping tips ranging from 0 to 10 mN (Fig. 3a). Analytical displacements were compared to those predicted by FEA and found to be on average ca. 10% greater: however, they do not take into account parasitic motion in *x* and *y* directions. Maximum stress, as expected, was found at the roots of the hot arms and suggest that the stiffness of the whole spring system will be around $180\ \mathrm{Nm}^{-1}$.

The effects of input voltage on the relative displacement of the gripper tips and of their temperature predicted from the FEA simulation are shown in Fig. 3(b). Maximum displacement was measured at the furthest tip of the micro-gripper arm. Input voltages were 0.1, 0.25, 0.5 and 1V leading to displacements varying from 35.2 µm to 524 µm. The tip temperature was kept low, the maximum increase was 18.7°C, Fig. 3c, i.e. the tip temperature was 43.7°C when the maximum voltage of 1V was applied. However, this voltage could never be reached in reality as the corresponding maximum temperature in the structure would be in excess of 600°C which is far above the glass transition temperature of SU-8, i.e. $T_g = 210°\mathrm{C}$, with degradation of the material initiating at ca. 315°C [22].

Micro-grippers were also modelled when operating in an aqueous medium to mimic cell culture: this was done by adjusting the surface heat transfer coefficient. For the same input voltages as before displacements were halved, convection to the surrounding fluid was increased and the tip temperature remained at a constant 25°C up to the maximum input voltage of 1 V. Gripping stiffness was investigated to ensure specimens could be held; this was done using substructing in ANSYS. Gripping force depends on the stroke of the micro-gripper arm and ranges from 100µN up to a maximum of 1mN.

Published in J. Micromech. Microeng. **23** (2013) 015005, doi:10.1088/0960-1317/23/1/015005

3. Experimental

The micro-grippers were fabricated on 76.4mm diameter, 200µm thick Si <110> wafer with 1µm thick insulation layer of SiO_2 which also improved the adhesion of SU-8 to the substrate. The process flow is shown in Fig. 4.

Aluminium was evaporated to a thickness of 600 nm at a rate of $\leq 1\,\mathrm{nm\,s^{-1}}$ and a pressure of $\leq 5\times 10^{-3}\,\mathrm{mbar}$ using an Edwards 305 evaporator. S1813 positive photoresist (Chestech Ltd., UK) was spin coated to a thickness of 1.3 µm. The wafer was then exposed to the anchor pattern for $100\,\mathrm{mJ\,cm^{-2}}$ using an OAI J500 photo aligner. The anchor pattern allows the SU-8 structure to adhere to the silicon substrate, the aluminium acts as a sacrificial support layer onto which the structure is patterned, it is removed at the end of the whole process. The S1813 was developed in a bath of MF351(Chestech Ltd., UK):deionized water at a dilution of 1:5 for 20s with gentle agitation, rinsed in DI water and dried with nitrogen. The aluminium anchor pattern was etched by placing the wafer in a beaker placed on a hotplate set to 60°C; the aluminium etchant $16H_3PO_4$+$1HNO_3$+$1CH_3COOH$+$1H_2O$ (Sigma Aldrich, UK) was pre-heated to 50°C and the wafer was immersed for 40s. The wafer was then rinsed in DI water for 10 min followed by quick acetone rinse to remove S1813 followed by a second DI water rinse and drying with nitrogen. Chromium (Kurt J Lesker, USA) was evaporated to a thickness of 100 nm at a rate $\leq 0.5\,\mathrm{nm\,s^{-1}}$; photoresist S1813 was spin coated as for the aluminium layer although the exposure dose was reduced to $82\,\mathrm{mJ\,cm^{-1}}$ to account for the smaller feature sizes present in the conduction path layer. This was developed in MF351 as previously described but for only 15 s and with gentle agitation. The wafer was then immersed in CR-14 Cr etchant (Compugraphics, UK) for 2 min with slight agitation at room temperature, rinsed as before after the aluminium etching and dried in nitrogen. SU-8 2007 was spin coated to the desired thickness (45 µm) and soft baked on a hotplate at 65°C for 1 min followed by 95°C for 4 mins; the wafer was removed from the hotplate and cooled for 10 mins to avoid residual stresses developing in the structure which could cause out of plane actuation during operation. The wafer was then exposed to UV light, of dose $280\,\mathrm{mJ\,cm^{-2}}$. The wafer was placed on the hotplate for post-exposure bake using the same times and temperatures as for the soft bake. The wafer was again cooled to reduce residual stresses before being immersed in a bath of EC solvent for 3 mins. The wafer was rinsed well using iso-propanol alcohol (IPA) and dried with nitrogen. To increase the strength of the micro-grippers the wafer was placed on the hotplate, now set at 145°C, to induce further cross linking in the polymer. The wafer was then finally cooled for at least 30 mins before the thickness of SU-8 layer was measured with a Dektak 3 surface profilometer.

The final stage was to release the aluminium sacrificial layer by immersing the wafer in a solution of 7.5 wt% potassium hydroxide (Sigma Aldrich, UK) for one hour after which the samples were removed, rinsed with IPA and dried in nitrogen. Samples were placed on the hotplate at 125°C to help with release through thermal shock and this resulted in around 70% of samples releasing successfully from the substrate with anchor points adhered. Electrical connection pads were enlarged using silver loaded electrically conductive paint (RS Components, UK) to allow for rapid electrical inspection of the samples. Wafers were cleaved along the <110> plane to allow complete release of the micro-gripper tips for micro-mechanical calibration and gripping trials.

Samples of the grippers were adhered to a simple circuit board designed using EasyPC and fabricated using a PCB milling machine (LPKF, Protomat C60). Electrically conductive paint was used to connect the conduction pads on the samples to conduction paths on the PCB which was placed on the main stage of a probe station for ease of moving samples underneath the microscope used for monitoring tip opening while they were tested using a suitable DC power supply.

4 Results and Discussion

4.1. Micro-gripper actuation

The micro-grippers showed repeatable actuation strokes from a few microns up to a maximum of 112 µm for a single arm, therefore showing a total tip opening of around 224 µm. However samples undergoing actuation greater than 100 µm showed fatigue and tended to fracture after a few strokes. Micro-grippers with a total actuation of less than 100 µm were operated for more than 50 cycles and showed little evidence of hysteresis on closing. Average resistance of the circuits was 2.34 W. Gripper opening as a function of electrical power consumption is shown in Fig. 5. The experimentally observed power consumption was greater than expected from FEA results. It must be noted the silicon substrate was not included in the FEA and further examination of the system using an infrared thermal imaging camera showed large heat transfer to the silicon substrate from the SU-8 resulting in the high power consumption observed. Once repeatable opening of micro-grippers was possible, they were tested closing around a number of fibres varying in diameter from 40 µm to 80 µm, see Fig. 6.

4.2. Micro-mechanical calibration

Micro-mechanical testing was carried out using two techniques. The performance of the folded flexures when under tension was investigated using a Tinius Olsen H5K-S test machine while the gripping stiffness of the overall device was examined using a Kleindiek micromanipulator and force measurement system (Fig. 7). Tensile tests of flexure springs were carried out until failure of the system occurred. Three groups of samples were tested with varying thicknesses of the active structural layer, viz. 30, 38 and 45 μm. In all the experiments linear stiffness was observed for values of the applied force up to 1.31±0.17, 1.67±0.10 and 2.04±0.41 mN respectively: at higher loads the material undergoes plastic deformation. Average stiffness for flexures of the three thicknesses were calculated by taking the gradient of the appropriate force-displacement curves and were $144\ \mathrm{N\,m^{-1}}$, $172\ \mathrm{N\,m^{-1}}$ and $200\ \mathrm{N\,m^{-1}}$ for SU-8 layer thicknesses 30, 38 and 45 μm respectively. Micro-mechanical FE models agreed well with experimental results for applied forces up to 2mN, results from the FE model with a structural layer thickness of 50 μm correlated well with the experimental results for a layer thicknesses measured to be 50 ± 5 μm (Fig. 7a). This can be explained by the dimensional inaccuracy from the fabrication processes in particular the beam junctions.

The Kleindiek force measuring system incorporates a fine positioning capability, which uses piezoelectric actuation, together with force sensing ability using a silicon piezo-resistive cantilever beam. The Kleindiek micromanipulator was controlled using NC Software (Kleindiek Nanotechnik) and data was collected using Labview via a NI 6009 data acquisition USB device. The force measuring system has a stiffness of ca. $2-4\ \mathrm{N\,m^{-1}}$. Micro-mechanical calibration was done under an optical microscope in plane with the gripping direction (Fig. 8). Ten samples with thicknesses of 24, 33.8 and 45 μm were tested and all showed good results with low standard deviation with gripping stiffness of 1.2, 1.61 and $2.14\ \mathrm{N\,m^{-1}}$ respectively (Fig 7b).

5. Conclusions

A fully integrated system capable of large, repeatable displacements with the ability to measure critical forces applied to small biological samples, such as fibrils, has been investigated. The polymer based gripper structure provides biocompatibility and the tests outlined above have demonstrated the aptitude of this design for repeatable small-scale tissue manipulation. The method described permits micro-grippers to be fabricated using low-cost photolithography without the need for dry etching. Although a fully working system with the ability to grip tissues and measure tensile forces has not been validated, each individual element has been shown to work and the concept has been proved. Large displacements of gripper arms are possible, up to 100 µm gap opening can occur in the elastic range of the grippers for up to 50 cycles; larger tip opening up to a maximum of 224 µm can be employed but resulted in fatigue limited operating cycles. The variable displacement capability allow variable forces to be applied to objects for manipulation, from a few µN up to 1 mN, a necessity when handling delicate biological samples. Variation in thickness of micro-grippers allows for slight variation in force resolution of the folded flexures in the range of 20-50 µN. Predictions from the finite element model correlated well with experimental results. Further work must be conducted to incorporate the micro-mirror to create a fully integrated system.

Acknowledgements

The authors are indebted to Ian Burnett of IDB Technologies and EPSRC for financial support and studentship for REM at the University of Dundee. Irene McMenanin of Compugraphics. Dr Gary Callon for technical support and microengineering advice.

References

1. Suresh S 2007 Biomechanics and biophysics of cancer cells *Acta Biomaterialia* **3** 413-438
2. Khodabukus A, Paxton J P, Donnelly K and Baar K 2007 Engineered muscle: a tool for studying muscle physiology and function *Exerc Sport Sci Rev.* **35** 186-9
3. Lee S, Zeiger A, Maloney J, Kotecki M, Van Vliet K J and Herman I M 2010 Pericyte actomyosin-mediated contraction at the cell-material interface can modulate the microvascular niche *Journal of Physics: Condensed Matter* **22**
4. Kim C, Pisano A P, Muller R S, Lim M G 1990 Polysilicon microgripper *Technical Digest IEEE Solid-State Sensor and Actuator Workshop* 48–51
5. Kim K, Liu X, Zhang Yand Sun Y 2008 Nanonewton force-controlled manipulation of biological cells using a monolithic MEMS microgripper with two-axis force feedback *J. Micromech and Microeng* **18** 055013
6. Lin G and Pister K S J 2000 Surface Micromachined polysilicon heart cell transducer *Journal of Microelectromech Systems* **9** 9-17
7. Menciassi A, Eisinberg A, Carrozza M C and Dario P 2003 Force sensing microinstrument for measuring tissue properties and pulse in micro-surgery *IEEE/ASME Trans Mechatron* **8** 10–17
8. Kohl M, Just E, Pfleging W and Miyazaki S 2000 SMA Microgripper with integrated antagonism *Sensors and Actuators A: Physical* **83** 208-213
9. Volland B E, Heerlein H and Rangelow I W 2002 Electrostatically driven microgripper *Microelectronic Engineering* **61** 1015-102
10. Xinhan H., Jianhua C, Min W and Xiadong L 2005 A piezoelectric bimorph micro-gripper with micro-force sensing *IEEE International Conference on Information Acquisition*
11. Nah S K and Zhong Z W 2007 A microgripper using piezoelectric actuation for micro-object manipulation *Sensors and Actuators A: Physical* **133** 218-224
12. Kohl M, Just E, Pfleging W and Miyazaki S 2000 SMA Microgripper with integrated antagonism *Sensors and Actuators A: Physical* **83** 208-213
13. Guckel H, Klein J, Christenson T, Skrobis K, Laudon M, Lovell E G 1992 Thermo-magnetic metal flexure actuators *Solid-State Sensor and Actuator Workshop, 5th Technical Digest*, 73-75
14. Pan C S and Hsu W 1997 An electro-thermally and laterally driven polysilicon microactuator *J. Micromech Microeng* **7** 7-13
15. Chronis N and Lee L P 2005 Electrothermally activated SU-8 microgripper for single cell manipulation in solution *J. Microelectromech Systems* **14** 857-863

16. Luo J K, Flewitt A J, Spearing S M , Fleck N A and Milne W I 2005 Comparison of microtweezers based on three lateral thermal actuator configurations *J. Micromech Microeng.* **15** 1294-1302

17. Mackay R E, Lionis N and Le H-R. 2011 3D Surface Topography and Reflectivity of Anisotropic Etched Silicon Micromirrors for BioMEMS *Microsystem Technol* **17** 1763-1770.

18. Lorenz H, Despont M, Fahrni N, LaBianca N, Renaud P, Vettiger P 1997 SU-8: a low-cost negative resist for MEMS *J. Micromech Microeng.* **7** 121-124

19. Lin L and Lin S H 1998 Vertically driven microactuators by electrothermal buckling effects *Sensors and Actuators A: Physical* **71** 35-39

20. Dellmann L Roth S Beuret C Racine GA Lorenz H Despont M Renaud P Vettiger P de Rooij NF 1997 Fabrication process of high aspect ratio elastic structures for piezoelectric motor applications *TRANSDUCERS '97 Chicago* **1** 641-644

21. Mackay R E, H-R, Keatch R P 2011 Design optimisation and fabrication of SU-8 based electro-thermal micro-grippers. *Journal of Micro-Nano Mechatronics* **6** 13-22

22. Dai W, Lian K and Wang W 2006 Design and fabrication of a SU-8 based electrostatic microactuator *Microsystem Technologies: HARMST, High Aspect Ratio Micro Structure Technology Workshop* **13** 271-277

Published in J. Micromech. Microeng. **23** (2013) 015005, doi:10.1088/0960-1317/23/1/015005

Figure captions

Fig. 1 Design concept of polymer micro-gripper fabricated on a silicon substrate. The gripping force is provided by thermal activation while the tensile force applied to the gripped specimen can be monitored via the lateral movement of the shuttle which is restrained by the folded flexure.

Fig. 2 Micro-gripper design.

Fig. 3 Finite Element results for SU-8 microgrippers: (a) Comparison of maximum displacement and hinge stress against applied force (b) displacement, maximum temperature and tip temperature in air; and (c) actuation and thermal flux plot with 2 µm width conduction path operated at 0.25 V.

Fig. 4 Process flow.

Fig. 5 Operating power consumption and total tip opening; comparison of FEA and experimental results.

Fig. 6 Micro-grippers holding (a) 45 µm diameter fibre (b) 75 µm diameter fibre.

Fig. 7 Microgripper stiffness results: (a) Spring stiffness of folded flexure system, comparison of FEA and experimental results. (b) Micro-gripper stiffness of tips for holding sample, stiffness of single arm 24 µm thickness measured stiffness 1.2 Nm^{-1}.

Fig. 8 Nano-mechanical calibration to find gripping stiffness.

Published in J. Micromech. Microeng. **23** (2013) 015005, doi:10.1088/0960-1317/23/1/015005

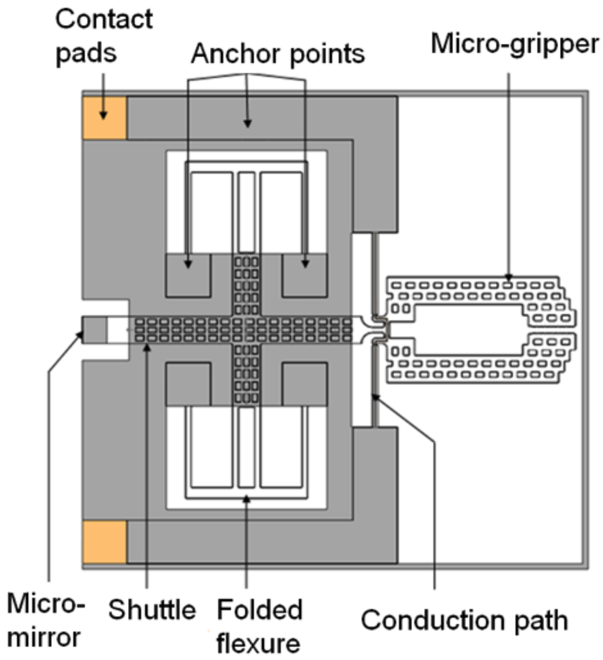

Figure 1. Design concept of polymer micro-gripper fabricated on a silicon substrate

Published in J. Micromech. Microeng. **23** (2013) 015005, doi:10.1088/0960-1317/23/1/015005

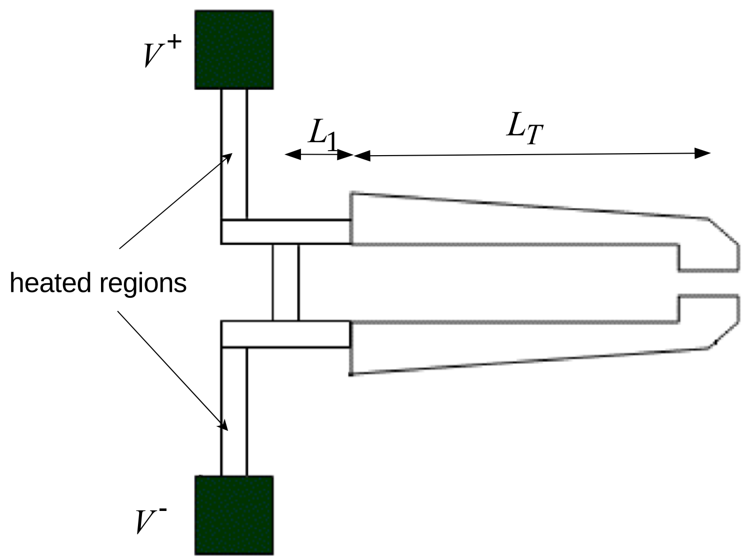

Figure 2. Micro-gripper design

Published in J. Micromech. Microeng. **23** (2013) 015005, doi:10.1088/0960-1317/23/1/015005

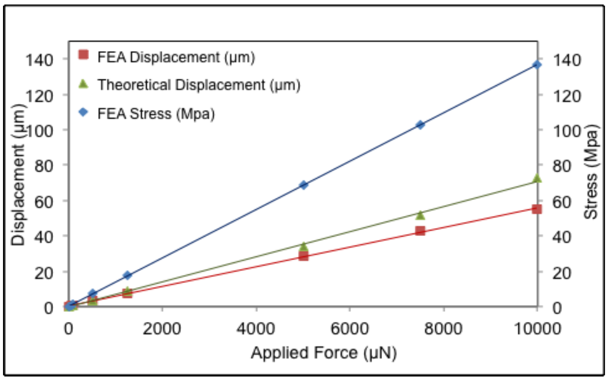

(a)

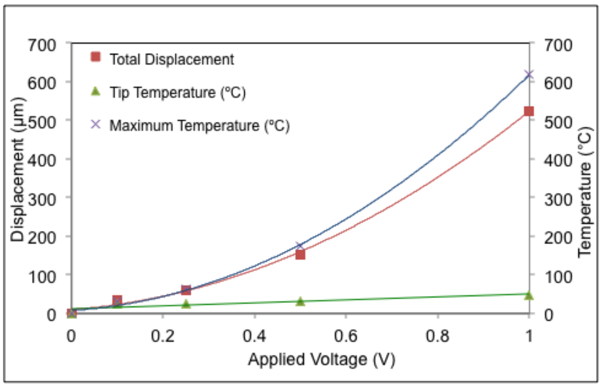

(b)

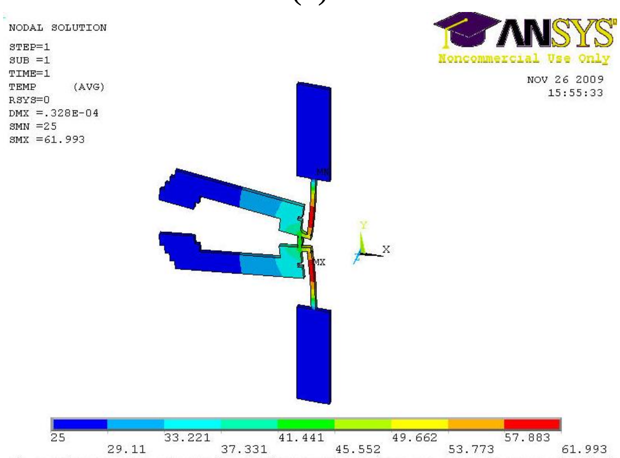

(c)

Figure 3. Finite Element results for SU-8 microgrippers: (a) Comparison of maximum displacement and hinge stress against applied force (b) displacement, maximum temperature and tip temperature in air; and (c) actuation and thermal flux plot with 2 μm width conduction path operated at 0.25 V.

Published in J. Micromech. Microeng. **23** (2013) 015005, doi:10.1088/0960-1317/23/1/015005

A: DSP (110) Si wafer 200 μm thick with 1 μm SiO_2

B: Evaporate 600 nm aluminium

C: Pattern Al to produce anchor points

D: Evaporate 100 nm Cr

E: Pattern chromium conduction path

F: Spin coat SU-8 2007

G: Pattern SU-8

H: Remove sacrificial layer in 7.5wt% KOH

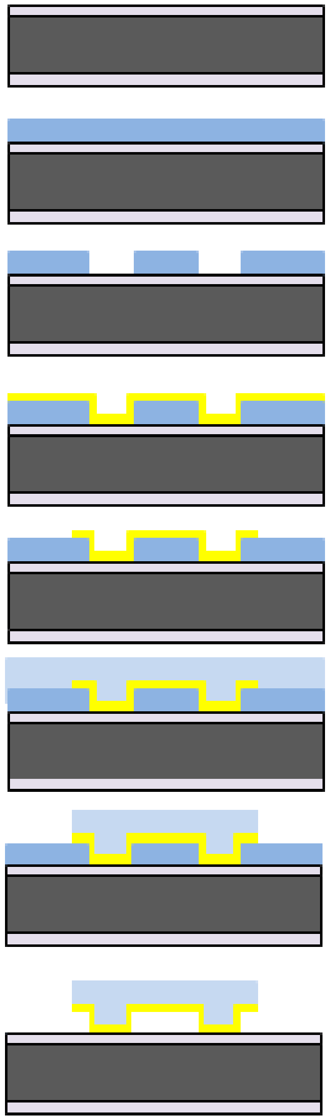

Figure 4. Process flow

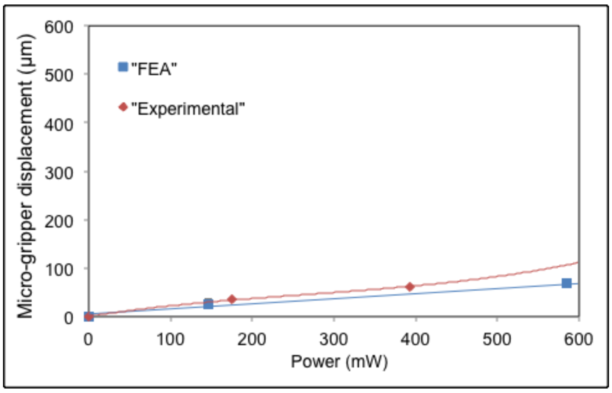

Figure 5. Operating power consumption and total tip opening; comparison of FEA and experimental results.

Published in J. Micromech. Microeng. **23** (2013) 015005, doi:10.1088/0960-1317/23/1/015005

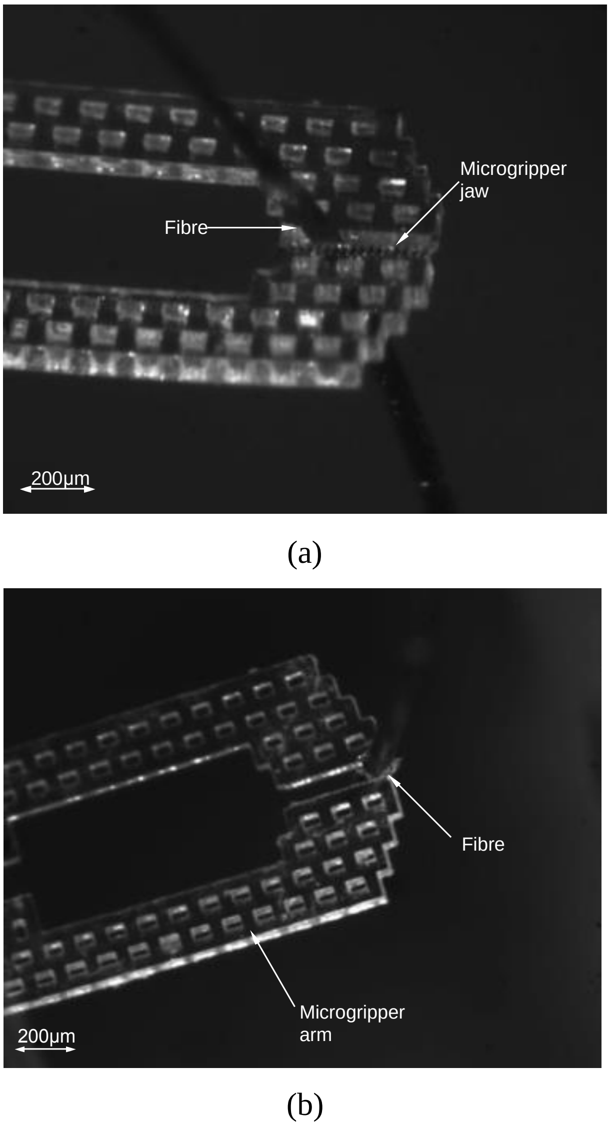

Figure 6. Micro-grippers holding (a) 45 μm diameter fibre (b) 75 μm diameter fibre.

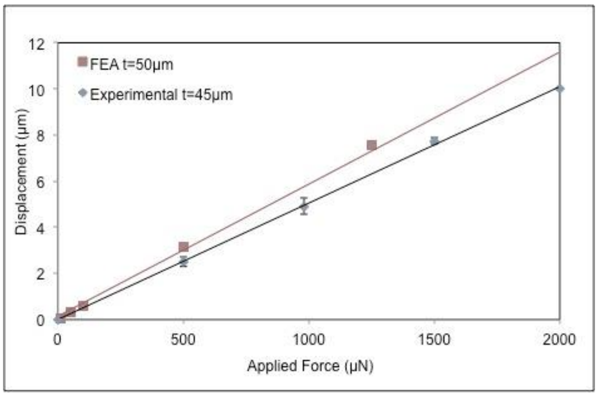

(a)

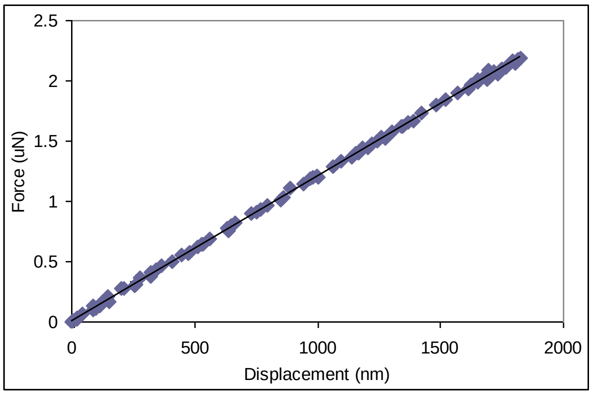

(b)

Figure 7. Microgripper stiffness results: (a) Spring stiffness of folded flexure system, comparison of FEA and experimental results. (b) Micro-gripper stiffness of tips for holding sample, stiffness of single arm 24 μm thickness measured stiffness 1.2 Nm^{-1}.

Published in J. Micromech. Microeng. **23** (2013) 015005, doi:10.1088/0960-1317/23/1/015005

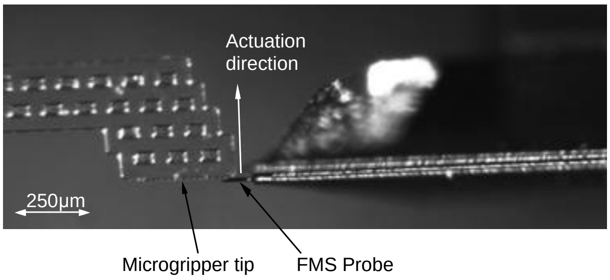

Figure 8. Nano-mechanical calibration to find gripping stiffness.